

respect to profiles and with respect to streamwise variations, and thus for providing the condition required to specify the shape parameters of the velocity profiles. The near constancy of the parameter β suggests that either of the two procedures just described for completing the system of equations for the direct problem will give equivalent results.

IV Conclusions

An analysis of the turbulent incompressible boundary layer with streamwise pressure gradients has been carried out. The analysis is applied to equilibrium and near-equilibrium flows, which have been obtained experimentally by others for adverse, zero, and favorable pressure gradients and which may be constructed numerically by application of the analysis. The results of these applications indicate that the suggestion of Clauser concerning the eddy viscosity in the outer layer incorporated in the present analysis provides a relatively simple, consistent, and accurate description of such flows. A means for determining the shape parameters of the velocity profiles for nonequilibrium flow is thus suggested.

References

- ¹ Clauser, F. H., "Turbulent boundary layers in adverse pressure gradients," *J. Aeronaut. Sci.* **21**, 91-108 (1954).
- ² Clauser, F. H., *The Turbulent Boundary Layer, Advances in Applied Mechanics* (Academic Press, New York, 1956), Vol. IV.
- ³ Coles, D., "The law of the wake in the turbulent boundary layer," *J. Fluid Mech.* **1**, 191-226 (1956).
- ⁴ Coles, D., "Remarks on the equilibrium turbulent boundary

layer," *J. Aeronaut. Sci.* **24**, 495-506 (1957).

⁵ Townsend, A. A., *The Structure of Turbulent Shear Flow* (Cambridge University Press, Cambridge, England, 1956).

⁶ Ferrari, C., 'Wall turbulence,' *Corso Sulla Teoria della Turbolenza* (Casa Editrice Cremonesi, Rome, 1957), Sec. C; also NASA RE2-8-59W (March 1959).

⁷ Coles, D. E., "The turbulent boundary layer in a compressible fluid," Rand Corp. Rept. R-403 PR (September 1962).

⁸ Spence, D. A., "The development of turbulent boundary layers," *J. Aeronaut. Sci.* **23**, 31-15 (1956).

⁹ Rotta, J. C., "The turbulent boundary layers in incompressible flow," *Progress in Aeronautical Sciences* (Pergamon Press, New York, 1962), Vol. 2, pp. 1-220.

¹⁰ Coles, D., "The law of the wall in turbulent shear flow," *Jahre Grenzschichtforsch.* **50**, 133-163 (1955).

¹¹ Tetervin, N. and Lin, C. C., "A general integral form of the boundary layer equations for incompressible flow with an application to the calculation of the separation point of turbulent boundary layers," NACA TN 2158 (1950).

¹² Ludwig, H. and Tillman, W., "Untersuchungen über die Wandschubspannung in Turbulenten Reibungsschichten," *Ingr.-Arch.* **17**, 288-299 (1949); also NACA TM 1285 (May 1950).

¹³ Libby, P. A., Baronti, P. O., and Napolitano, L., "A study of the turbulent boundary layer with pressure gradient, Part I, General analysis and equilibrium flows for incompressible fluids," General Applied Sci. Labs. Rept. 333 (February 1963).

¹⁴ Coles, D., "Measurements in the boundary layer on a smooth flat plate in supersonic flow, 1—The problem of the turbulent boundary layers," Jet Propulsion Lab., Calif. Inst. Tech. Rept. 20-69 (June 1, 1953).

¹⁵ Wieghardt, K. and Tillman, W., "Zur Turbulenten Reibungsschicht Druckanstieg," *Deut. Luftfahrtforsch.* UM 6617 (November 20, 1944); also NACA TM 1314 (October 1951).

¹⁶ Bauer, W. J., "The development of the turbulent boundary layer on steep slopes," *Proc. Am. Soc. Civil Engrs.* **79**, no. 281, 1-25 (1953).

MARCH 1964

AIAA JOURNAL

VOL. 2, NO. 3

Nonequilibrium Hypersonic Flat-Plate Boundary-Layer Flow with a Strong Induced Pressure Field

GEORGE R. INGER*

Aerospace Corporation, El Segundo, Calif.

This paper presents a theoretical study of the effect of a strong self-induced pressure field on nonequilibrium hypersonic boundary-layer flow along a sharp flat plate in a dissociating diatomic gas. An analytical solution for the nearly frozen flow near the leading edge is presented which explicitly shows the effects of the induced pressure field in the case of strong interaction, including the back effect of the growing dissociation level on the induced pressure field itself. An approximate solution is also given for the entire nonequilibrium flow regime. The numerical results of the theory show that the induced pressure field can increase the degree of dissociation over a 10-ft run of plate by a factor of three to four or more at hypersonic flight conditions of practical interest. These results also suggest that the fully viscous flow region very near the leading edge can play an important part in determining the nonequilibrium dissociation history along the plate when the induced pressure field is taken into account.

Nomenclature

A = dissociation rate parameter
 C_∞ = Chapman-Rubens constant
 \bar{c}_p = frozen specific heat of mixture

D = dissociation rate distribution function [Eqs. (6) and (8)]
 F^* = function defined in Eq. (54)
 f = boundary-layer stream function
 G = parameter in fully viscous flow theory [Eq. (57)]
 g = h/h
 g_w = $\bar{c}_p T_w / h$
 H_∞ = $2\alpha_\infty h_D / u_\infty^2$
 h_D = specific molecular dissociation energy
 h = total enthalpy
 I = integral in displacement thickness relation [Eqs. (11) and (14)]

Presented as Preprint 63-442 at the AIAA Conference on Physics of Entry into Planetary Atmospheres, Cambridge, Mass. August 26-28, 1963; revision received January 3, 1964.

* Member, Technical Staff, Aerodynamics and Propulsion Research Laboratory. Member AIAA.

I	= nonequilibrium flow displacement thickness integrals [Eq (46)]
$g(\eta)$	= reaction rate integral defined by Eq (43)
j	= switching function defined by Eq (33)
K^*	= $M_\infty(d\delta^*/dx)$
k_D, k_R	= dissociation and recombination rate coefficients, respectively
k'	= recombination rate constant
$\mathcal{K}(T)$	= equilibrium parameter
Le	= Lewis number
M_∞	= freestream Mach number
$n(x)$	= function defined by Eq (13)
Pr	= Prandtl number
P_I	= induced pressure perturbation due to nonequilibrium dissociation [Eq (26)]
p	= static pressure
p_t	= standard atmospheric pressure
$p_{0,F}$	= constant defined by Eq (38)
Q_w	= $[2/\xi_0]^{1/2}(2\dot{q}_w/u_\infty^2)$
\dot{q}_w	= heat-transfer rate
R	= recombination rate distribution function [Eqs (6) and (9)]
$Re_{\infty, x}$	= $\rho_\infty u_\infty x / \mu_\infty$ (local Reynolds number based on free-stream conditions)
R_M	= molecular gas constant
R_u	= universal gas constant
S	= dissociation rate parameter
$s(\eta)$	= solution to Eq (39)
$\bar{s}(\eta^*)$	= parameter defined by Eq (50)
T	= absolute temperature
T_D	= molecular dissociation temperature
T_0	= total temperature, $T_\infty + u_\infty^2/2\bar{c}_p$
T_1, T_2	= reference temperatures in reaction rate
u	= velocity component parallel to freestream direction
$V_s(\eta)$	= $v(\eta)/v(\infty)$
$v(\eta)$	= function defined by Eq (42a)
\dot{w}_A	= net volumetric rate of atom mass production [Eq (5)]
x, y	= coordinates parallel and normal to plate respectively
z_F	= function defined by Eq (29)
α	= atom mass fraction
β^*	= parameter defined by Eq (45)
Γ	= characteristic (flow time/dissociation time) parameter [Eq (7)]

Introduction

BOUNDARY-LAYER induced pressure fields have been heretofore neglected in analyses of nonequilibrium-dissociated and ionized boundary-layer flows around slender aerodynamic bodies. Previous investigations concerning the interaction between an induced pressure field and high-temperature real gas effects have been confined to the limiting cases of either chemically frozen or completely equilibrium dissociated gas flows.^{1,2} However, strong self-induced pressures near the leading edge of such bodies do exist in just those low Reynolds number flight regimes which also favor a substantial departure from equilibrium within the boundary layer over an appreciable extent of the body. Therefore, since the early dissociation and ionization rates in the nonequilibrium boundary layer increase directly as the pressure, neglect of the induced pressure field could significantly underestimate the degree of dissociation and ionization in the flow field surrounding high-altitude re-entry bodies.

To obtain some insight into this problem, this paper presents a theory of the nonequilibrium hypersonic boundary layer along a sharp flat plate in the presence of a strong self-induced pressure field for the case of a dissociating diatomic gas. The analysis employs the usual boundary-layer equations in conjunction with a first-order, strong interaction model of the induced pressure field based on hypersonic small-disturbance theory. This approach is a logical first step in appraising both the effect of induced pressure fields on the nonequilibrium boundary layer around slender aerodynamic bodies and the possible influence of the fully viscous flow region very near the leading edge on this nonequilibrium flow.

The simplifying assumptions and basic formulation of the problem are first given for either a completely catalytic or perfectly noncatalytic plate surface. Then, based on the fact that atom recombination has a negligible effect on the nonequilibrium relaxation in the boundary layer except very near equilibrium,^{3,4} an analytical solution is obtained which describes the nonsimilar chemical behavior for nearly frozen flow along the plate. By taking advantage of the exponential dependence of the dissociation rate on the temperature, a simple, closed-form approximation to this first-order solution is also derived. Furthermore, an approximate solution is given for arbitrary reaction rate (including recombination) throughout the nonequilibrium flow regime by performing a nonlinear, local extrapolation of the nearly frozen solution. Numerical examples of the theory for representative hypersonic flight conditions are then presented and discussed. Finally, the significance of the fully viscous region very near the plate leading edge will be examined in connection with these results.

Formulation of the Problem

Consider laminar nonequilibrium boundary-layer flow along a sharp flat plate immersed at zero angle of attack in a hypersonic stream of diatomic gas. The plate has a uniform but arbitrary wall temperature and is either completely catalytic or perfectly noncatalytic with respect to heterogeneous atom recombination on the surface. The shock envelope and the outer edge of the boundary layer are assumed to be separated by a thin, nonreacting layer of inviscid small-disturbance hypersonic flow ($u \simeq u_\infty$, $\sin^2 \sigma \ll 1$, $\alpha = \alpha_\infty$, $\tilde{\gamma} = \tilde{\gamma}_\infty$). This assumption clearly breaks down sufficiently close to the leading edge, where the entire shock layer becomes fully viscous; the resulting limitations on the present analysis are discussed below. With respect to the flow in the boundary layer, one adopts as a matter of convenience the frequently employed simplifying assumptions $Pr = Le = 1$, $\rho\mu = \text{const} = \rho_A\mu_A = \rho_\infty\mu_\infty C_\infty(p_A/p_\infty)$, where C_∞ is the Chapman-Rubens constant, and $\bar{c}_p = \text{const}$. Moreover, following other investigators,⁵⁻⁷ the pressure gradient term in the momentum equation is neglected, and the velocity profile is taken to be independent of the solution to the energy and species conservation equations. This approximation, which can be justified theoretically when either the shock density ratio ρ_∞/ρ is very small^{7,8} or the wall is highly cooled,^{5,6} has but a minor effect on the nonequilibrium reaction effects of interest here.

In terms of the well-known similarity coordinates

$$\eta = \frac{u_e}{[2\xi]^{1/2}} \int_0^y \rho dy \quad (1)$$

$$\xi = \rho_\infty \mu_\infty C_\infty u_\infty \int_0^x \frac{p_e}{p_\infty} dx \equiv \xi_0 \int_0^x \frac{p}{p_\infty} dx$$

the governing diffusion and energy equations for a nonequilibrium-dissociating boundary layer of diatomic gas can be written under the foregoing assumptions as

$$f \frac{\partial \alpha}{\partial \eta} + \frac{\partial^2 \alpha}{\partial \eta^2} - 2f' \xi \frac{\partial \alpha}{\partial \xi} = - \frac{2\xi}{\partial \xi / \partial x} \left(\frac{\dot{w}_A}{\rho} \right) \quad (2)$$

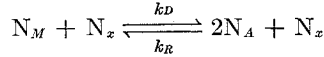
$$f \frac{\partial g}{\partial \eta} + \frac{\partial^2 g}{\partial \eta^2} - 2f' \xi \frac{\partial g}{\partial \xi} = 0 \quad (3)$$

where

$$g \equiv \frac{h_s}{h} = \frac{\bar{c}_p T + \alpha h_D + (u_\infty^2/2)(f')^2}{\bar{c}_p T + \alpha_\infty h_D + u_\infty^2/2} \quad (4)$$

is the nondimensionalized total enthalpy, $f(\eta)$ is the Blasius function [$f'(\eta) = u/u$], and \dot{w}_A is the net volumetric rate of atom mass production due to chemical reaction. Taking the chemical kinetics of a dissociating diatomic gas to follow

the reaction



where N_M , N_A , and N_x denote the number of moles of molecules, atoms, and inert third-body collision partners, respectively, application of the laws of phenomenological rate kinetics⁹ yields

$$\frac{\dot{w}_A}{\rho} = 4k_R \left(\frac{p}{\rho_u T} \right)^2 \left[\frac{(1 - \alpha)K(T)}{4(p/p_\infty)} - \frac{\alpha^2}{1 + \alpha} \right] \quad (5)$$

Then letting the recombination rate k_R and the equilibrium parameter $K(T)$ be of the general form^{10, 11}

$$k_R = k_R' \left(\frac{T}{T_{R1}} \right)^\omega$$

$$K(T) = A \left(\frac{T}{T_{R2}} \right)^S \exp \left(- \frac{T_D}{T} \right)$$

where k_R' , ω , A , and S are constants, T_{R1} and T_{R2} are constant reference temperatures, and $T_D = h_D/\mathcal{R}_M$ is the characteristic molecular-dissociation temperature, the reaction term on the right side of Eq. (2) becomes

$$- \frac{2\xi}{d\xi/dx} \left(\frac{\dot{w}_A}{\rho} \right) = -\Gamma(\xi) \left[D(\alpha, T) - R \left(\alpha, T, \frac{p_e}{p_\infty} \right) \right] \quad (6)$$

with

$$\Gamma(\xi) = \frac{2k_R'(p_{at}/\mathcal{R}_M)^2(p_\infty/p_{at})A}{T_{R1}^2 u_\infty} \frac{\xi}{\xi_0} \equiv \Gamma_0 \frac{\xi}{\xi_0} \quad (7)$$

$$D(\alpha, T) = (1 - \alpha) \left(\frac{T}{T_{R1}} \right)^{\omega-2} \left(\frac{T}{T_{R2}} \right)^S \exp \left(- \frac{T_D}{T} \right) \quad (8)$$

$$R \left(\alpha, T, \frac{p_e}{p_\infty} \right) = \frac{4p_\infty/p_{at}}{A} \left(\frac{\alpha^2}{1 + \alpha} \right) \left(\frac{T}{T_{R1}} \right)^{\omega-2} \frac{p_e}{p_\infty} \quad (9)$$

The parameter $\Gamma(\xi)$ is a characteristic local (convection time/dissociation time) ratio for the boundary layer and is seen to be directly proportional to the transformed streamwise coordinate ξ along the plate. The function D represents the dissociation-rate distribution across the boundary layer and, as defined here, is independent of the local pressure. The function R represents the corresponding recombination-rate distribution, being proportional to α^2 and the local pressure. These functions have the important property that $D = R$ in the limiting case of equilibrium flow. However, R is negligible in comparison to D throughout most of the nonequilibrium boundary-layer flow regime along the plate except very close to equilibrium.

The boundary conditions to be imposed on the solution to the foregoing equations are as follows: at the outer edge of the boundary layer, $\alpha(\infty, \xi) = \alpha_\infty$, $g(\infty, \xi) = 1$, and $f'(\infty) = 1$; and at the body surface, $f(0) = f'(0) = 0$, $T(0, \xi) = T_w = \text{const}$, and either $\alpha(0, \xi) = 0$ with $g(0, \xi) = \bar{c}_p T_w/h_{se} \equiv g_w$ for a completely catalytic surface† or $(\partial\alpha/\partial\eta)(0, \xi) = 0$ with $g(0, \xi) = g_w + \alpha(0, \xi)h_D/h_{se}$ unknown for the opposite extreme of a perfectly noncatalytic surface. In terms of the total enthalpy profile, the heat-transfer rate \dot{q}_w is given by the expression

$$\frac{2\dot{q}_w/u_\infty^2}{(\xi_0/2)^{1/2}} \equiv Q_w = \frac{p_e/p_\infty}{(\xi/\xi_0)^{1/2}} (1 + H_\infty) \frac{\partial g}{\partial \eta}(0, \xi) \quad (10)$$

where $H_\infty \equiv 2\alpha_\infty h_D/u_\infty^2$.

Formulation of the problem is completed by specifying the displacement-thickness distribution $\delta^*(x)$ of the nonequilibrium

boundary layer and an appropriate relationship between the induced pressure field and $d\delta^*/dx$. Consistent with the assumption of a small-disturbance, hypersonic inviscid flow, the following expression for $d\delta^*/dx$ can be derived from the basic definition

$$\rho u \delta^* \equiv \int_0^y (\rho u - \rho u) dy$$

upon neglecting the effect of molecular weight variation on ρ/ρ (which is small in the present study) and using both the thermal equation of state and Eq. (4),

$$M_\infty \frac{d\delta^*}{dx} \equiv K^* = \left(\frac{\bar{\gamma}_\infty - 1}{2} \right) \bar{\chi}_\infty \left[\frac{\phi(x)}{2p/p_\infty} \right]^{1/2} I(x) \times$$

$$\left[1 + n(x) + \frac{x}{\phi} \frac{d\phi}{dx} + \frac{2x}{I} \frac{dI}{dx} \right] \quad (11)$$

where $\bar{\gamma}$ is the frozen specific heat ratio, $\bar{\chi}_\infty = M_\infty^3 (C_\infty/Re_{\infty x})^{1/2}$ is the usual viscous interaction parameter,

$$\phi(x) \equiv \frac{\int_0^x \frac{p_e}{p_\infty} dx}{\frac{p_e}{p_\infty} x} \quad (12)$$

$$n(x) \equiv - \frac{X}{p} \frac{dp_e}{dx} \quad (13)$$

$$I = (1 + H_\infty) \int_0^\infty [g - (f')^2] d\eta -$$

$$H_\infty \int_0^\infty [1 - (f')^2] d\eta - \frac{2h_D}{u_\infty^2} \int_0^\infty (\alpha - \alpha_\infty) d\eta \quad (14)$$

The function I contains the combined effects of viscous dissipation heating, inviscid flow dissociation, and nonequilibrium dissociation within the boundary layer on the local mass flow deficiency due to the boundary layer. The local pressure field will be related to $d\delta^*/dx$ by the tangent wedge approximation for the hypersonic small-disturbance inviscid flow. In particular, for the case of strong interaction ($K^* \gg 1$) that is of prime interest here, this relation takes the form following¹²:

$$\frac{p_e}{p_\infty} \simeq 1 + \frac{\bar{\gamma}_\infty(\bar{\gamma}_\infty + 1)}{2} (K^*)^2 \quad (15)$$

Now, Eq. (15) underestimates the induced pressure in the region of moderate-to-weak interaction [$(p/p_\infty) - 1 \lesssim 0(1)$] downstream of the leading edge, since it neglects terms of order K^* , which eventually become important in this region. However, this is of minor consequence for the present purpose, since it will be seen that the significant effects of the induced pressure field on the nonequilibrium relaxation in the boundary layer occur almost entirely in the strong interaction region.

The general solution to Eqs. (2, 3, 6, 11, and 15) is a formidable mathematical task, involving a two-point boundary-value problem for two partial differential equations (one of which is highly nonlinear) that is coupled to a set of nonlinear ordinary differential equations. Even if one reduces Eqs. (2) and (3) to ordinary differential equations by assuming local similarity for the nonequilibrium boundary layer (i.e., neglecting the $\partial/\partial\xi$ terms a priori), a numerical solution on a digital computer is still required. However, a very useful insight to the main physical features of the problem can be obtained by first studying the case of nearly frozen nonequilibrium flow, where an analytical solution can be obtained. Moreover, this nearly frozen flow analysis also can be used in constructing an approximate, local nonequilibrium solution for arbitrary values of the reaction rate

† The heterogeneous dissociation rate on the surface is assumed negligible in comparison to the corresponding heterogeneous recombination rate.

Nearly Frozen Nonequilibrium Flow

Dissociation within the hypersonic boundary layer along the plate is instigated by the high temperatures resulting from viscous dissipation heating. At the leading edge where the boundary layer is chemically frozen, there exists an initial distribution of the dissociation rate per unit distance along the plate (with a pronounced maximum at the maximum frozen temperature), which initiates a dissociative relaxation toward equilibrium with increasing distance downstream of the leading edge. The recombination rate across the boundary layer in this highly nonequilibrium flow region is completely negligible by comparison unless α_∞ is extremely close to unity.

Series Method

Sufficiently near the leading edge, where the deviations from chemically frozen flow are small, the effect of chemical reaction on the boundary layer is related to the dissociation-rate distribution based on frozen-flow conditions and directly proportional to the local nonequilibrium flow parameter $\Gamma(\xi)^4$. Therefore, one can assume solutions to Eqs (2) and (3) of the form

$$\alpha(\eta, \xi) = \alpha_F(\eta) + \Gamma(\xi)\alpha_I(\eta) \quad (16a)$$

$$g(\eta, \xi) = g_F(\eta) + \Gamma(\xi)g_I(\eta) \quad (16b)$$

$$T(\eta, \xi) = T_F(\eta) + \Gamma(\xi)T_I(\eta) \quad (16c)$$

where the subscripts F and I denote the frozen-flow solution and the first-order perturbations due to nonequilibrium reaction, respectively. By substituting Eqs (16) into Eqs (2) and (3), equating to zero the net coefficient of each power of Γ , dropping second- and higher-order terms in Γ , and neglecting the effect of gas-phase recombination, one obtains the following two sets of relations governing the frozen-flow and the first-order reaction perturbations, respectively:

$$f\alpha_F' + \alpha_F'' = 0 \quad (17)$$

$$fg_F' + g_F'' = 0 \quad (18)$$

with

$$T_F = T g_F + \frac{h_D}{\bar{c}_p} (\alpha_\infty g_F - \alpha_F) + \frac{u_\infty^2}{2\bar{c}_p} [g - (f')^2] \quad (19)$$

$$f\alpha_I' + \alpha_I'' - 2f'\alpha_I = -D_F(\alpha_F, T_F) \quad (20)$$

$$fg_I' + g_I'' - 2f'g_I = 0 \quad (21)$$

with

$$T_I = (h g_I - h_D \alpha_I / \bar{c}_p) \quad (22)$$

The corresponding boundary conditions become $\alpha_F(\infty) = \alpha_\infty$, $g_F(\infty) = 1$, $\alpha_I(\infty) = g_I(\infty) = T_I(\infty) = 0$ with either $\alpha_F(0) = \alpha_I(0) = 0$ or $\alpha_F'(0) = \alpha_I'(0) = 0$. Also, for a fixed wall temperature T_w , one has $T_F(0) = T_w$, $g_F(0) = g_w + \alpha_F(0)h_D/h$, $T_I(0) = 0$, and $g_I(0) = \alpha_I(0)h_D/h$.

It should be noted that the equations governing the first-order nonequilibrium effects do not involve the local pressure and can, therefore, be solved independently of the particular relationship, such as (15), assumed in calculating p_e/p_∞ . This fortunate situation arises from the fact that the entire effect of the pressure field on the boundary-layer reaction rate for nearly frozen flow is implicit in the coordinate ξ when gas-phase recombination is neglected. Therefore, since $\Gamma \sim \xi$ and $\xi(\partial/\partial\xi) \sim \Gamma$, the pressure simply cancels out (residing solely in Γ) in obtaining Eqs (20) and (21).

Relations governing the induced pressure field for strong interaction, including the first-order back effect of nonequilibrium dissociation within the boundary layer, can now be derived. First, by substituting expansions (16a) and (16b)

into Eq (14), the displacement-thickness integral I can be written as

$$I = I_F + \Gamma I_I \quad (23)$$

where

$$I_F = (1 + H_\infty) \int_0^\infty [g_F - (f')^2] d\eta - H_\infty \int_0^\infty [1 - (f')^2] d\eta - \frac{2h_D}{u_\infty^2} \int_0^\infty (\alpha_F - \alpha_\infty) d\eta \quad (24a)$$

$$I_I = (1 + H_\infty) \int_0^\infty g_I d\eta - \frac{2h_D}{u_\infty^2} \int_0^\infty \alpha_I d\eta \quad (24b)$$

are constants, which can be evaluated once Eqs (17–21) are solved. Then, by analogy with Eqs (16) and (23), one assumes solutions for K^* and p/p_∞ of the form

$$K^* = K_F^* \left[1 + K_I^* \frac{I_I}{I_F} \Gamma \right] \quad (25)$$

$$\frac{p_e}{p_\infty} = \left(\frac{p_e}{p_\infty} \right)_F \left(1 + P_I \frac{I_I}{I_F} \right) \quad (26)$$

where K_I^* and P_I depend on the frozen-flow solution. Substituting Eqs (25) and (26) into (11) and (15) and dropping second and higher terms in Γ , the following two sets of relations governing the frozen boundary-layer induced pressure field and the nonequilibrium perturbation thereof, respectively, are obtained:

$$K_F^* \approx \left(\frac{\tilde{\gamma}_\infty - 1}{2} \right) \tilde{\chi}_\infty \left[\frac{\phi_F}{2(p/p_\infty)} \right]^{1/2} (1 + n_F) I_F \quad (27a)$$

$$\left(\frac{p_e}{p_\infty} \right)_F \approx 1 + \frac{\tilde{\gamma}_\infty(\tilde{\gamma}_\infty + 1)}{2} (K_F^*)^2 \quad (27b)$$

$$K_I^* = \frac{(p_e/p_\infty)_F P_I}{\tilde{\gamma}_\infty(\tilde{\gamma}_\infty + 1)(K_F^*)^2} \quad (28a)$$

$$P_I = \left[\frac{(1 + n_F)(p_e/p_\infty)_F}{(3 - n_F)\tilde{\gamma}_\infty(\tilde{\gamma}_\infty + 1)(K_F^*)^2} + 1 - \frac{z_F}{2} \right]^{-1} \quad (28b)$$

where

$$z_F \equiv \frac{\int_0^x \left(\frac{p_e}{p_\infty} \right)_F^2 x dx}{\left(\frac{p_e}{p_\infty} \right)_F x \int_0^x \left(\frac{p_e}{p_\infty} \right)_F dx} \quad (29)$$

Corresponding to the pressure field (26), it is also found that

$$\phi = \phi_F [1 + (1 - z_F) P_I (I_I/I_F) \Gamma] \quad (30)$$

$$\left. \begin{aligned} \Gamma &= \Gamma_F [1 + \Gamma_F z_F P_I (I_I/I_F)] \\ \Gamma_F &\equiv \Gamma_0 \phi_F (p/p_\infty) x \end{aligned} \right\} \quad (31)$$

which prove useful later. Note that, in deriving Eqs (28, 30, and 31), the parameters ϕ_F , n_F , and z_F were each taken to be constant. This is indeed exact in the limit of strong interaction ($\tilde{\chi}_\infty \gg 1$) and also remains a good approximation even for arbitrary values of $\tilde{\chi}_\infty$, since these parameters are rather slowly varying functions of x in the general case.^{13, 14}

Finally, the heat transfer to the plate can be written to first order in Γ upon substitution of Eqs (16b, 26, and 30) into (10) as

$$Q_w = (1 + H_\infty) \left[\frac{(p_e/p_\infty)_F}{\phi_F x} \right]^{1/2} \left\{ g_F'(0) + \Gamma \left[g_I'(0) + \left(\frac{2 - z_F}{2} \right) P_I g_I'(0) \frac{I_I}{I_F} \right] \right\} \quad (32)$$

The two terms inside the square bracket multiplying Γ repre-

sent the first-order effect of nonequilibrium reaction on the enthalpy profile, and the influence of the corresponding back effect of this reaction on the induced pressure field, respectively

Frozen-Flow Solution

Solutions to Eqs (17) and (18) for the stipulated boundary conditions are easily obtained by direct integration. Noting that $f'' + f''' = 0$, the atom concentration distribution is found to be

$$\alpha_F(\eta) = \alpha_\infty [1 - j + jf'(\eta)] \quad (33)$$

where $j = 0$ for a noncatalytic wall and $j = 1$ for a completely catalytic wall. The corresponding total enthalpy profile is

$$g_F(\eta) = g + (1 - g_w)f' + (h_D/h)(1 - f')\alpha_F(0) \quad (34)$$

Then, for a fixed wall temperature, Eq (19) yields

$$T_F(\eta) = T_w + (T - T_w)f' + (u_\infty^2/2\bar{c}_p)f'(1 - f') \quad (35)$$

regardless of the surface catalyticity ‡. For hypersonic flow, this temperature profile yields a dissociation-rate distribution that is mainly concentrated in a rather narrow band centered on the position $\eta = \eta^*$ of the maximum in the frozen temperature profile,⁴⁻¹⁴ the value of η^* given by

$$f'(\eta^*) = \frac{1}{2} + \frac{\bar{c}_p(T_e - T_w)}{u_\infty^2}, \quad f'(\eta^*) < 1 \quad (36)$$

Turning to the calculation of the self-induced pressure field acting on the frozen boundary layer, one first evaluates the displacement-thickness integral I_F from solutions (33) and (34) with the following result⁷:

$$\left. \begin{aligned} I_F &= \int_0^\infty f'(1 - f')d\eta + \frac{2\bar{c}_p T}{u_\infty^2} \int_0^\infty (1 - f')d\eta \\ &= 0.470 + 1.220 \left(\frac{2\bar{c}_p T_w}{u_\infty^2} \right) \end{aligned} \right\} \quad (37)$$

To the present order of approximation, this relation gives no effect of surface catalyticity on the induced pressure field, regardless of the inviscid flow dissociation level. Now, the algebraic Eqs (27) can be solved for with the following result in the strong interaction case:

$$\left(\frac{p_e}{p_\infty} \right)_F \simeq 1 + \frac{3}{8} (\bar{\gamma}_\infty - 1) [2\bar{\gamma}_\infty (\bar{\gamma}_\infty + 1)]^{1/2} I_F \bar{\chi}_\infty \equiv 1 + p_0 F \bar{\chi}_\infty \quad (38)$$

which in the limit $\bar{\chi}_\infty \gg 1$ agrees with the result given by the first-order strong interaction theory in Hayes and Probstein¹² for a perfect gas

First-Order Solution

Equation (20) governing the first-order nonequilibrium atom concentration and total enthalpy perturbations within the boundary layer has been previously treated in analyses of the nonequilibrium problem for the flat plate without an induced pressure field.⁴⁻¹⁵ The solutions are readily obtained by standard methods in terms of the known solution $s(\eta)$ to the associated homogeneous equation

$$fs' + s'' - 2f's = 0 \quad (39)$$

with $s(0) = 1$ and $s'(0) = 0$. These solutions are

$$\alpha_I(\eta) = s(\eta) \{ [1 - j + jV(\eta)]g(\infty) - g(\eta) \} \quad (40)$$

‡ Here, to be consistent with the hypersonic small disturbance approximations and chemically frozen-flow conditions employed one must take $T = T_\infty$.

$$g_I(\eta) = (h_D/h) \alpha_I(0) s(\eta) [1 - V(\eta)] \quad (41)$$

where

$$v(\eta) \equiv \int_0^\eta f''(\eta) s(\eta)^{-2} d\eta \quad (42a)$$

$$V(\eta) \equiv \frac{v_s(\eta)}{v(\infty)} \quad (42b)$$

$$g(\eta) \equiv \int_0^\eta \frac{f''(\eta)}{s^2(\eta)} \left[\int_0^\eta \frac{s(\eta) D_F(\eta) d\eta}{f''(\eta)} \right] d\eta \quad (43)$$

Plots of $s(\eta)$ and $v(\eta)$ can be found in Ref. 4. Calculation of some typical distributions of the normalized reaction-rate integral $g(\eta)/g(\infty)$ has shown that this ratio is relatively unaffected by the details of the reaction-rate distribution.¹⁴ Moreover, it was found that unless the freestream is very highly dissociated or $T_w/T_0 \gtrsim 0.25$ with $\alpha_\infty > 0$, it may be taken as independent of the surface catalyticity.

It has been pointed out in Ref. 4 that very useful closed-form approximations to the over-all reaction-rate integrals $g(\infty)$ and $g(\eta^*)$ can be obtained by the method of steepest descent¹⁶ for highly dissipative boundary-layer flows with a pronounced temperature maximum in the boundary layer. Expanding Eq (43) into two single integrals with an integration by parts, and then using this method in evaluating the integrals (see Ref. 4 for details), one can obtain the following analytical expressions:

$$g(\eta^*) \simeq 0 \quad (44a)$$

$$\left. \begin{aligned} g(\infty) &\simeq \pi^{1/2} \beta^* \frac{s(\eta^*)}{f''(\eta^*)} [v(\infty) - \\ &\quad v(\eta^*)] \left[\frac{1 + \text{erf}(\eta^*/\beta^*)}{2} \right] D_F(\eta^*) \\ &\equiv F^* D_F(\eta^*) \end{aligned} \right\} \quad (44b)$$

where

$$\beta^* \equiv \left(\frac{2\bar{c}_p}{T_D} \right)^{1/2} \frac{T_F(\eta^*)}{f''(\eta^*) u_\infty} \quad (45)$$

Equation (44b) can be thought of as representing the over-all reaction-rate integral by the product of the dissociation rate at the maximum frozen temperature and a form factor F^* accounting for the integrated effect of reaction across the boundary layer as modified by convection and diffusion. Comparison with exact numerical values shows that this approximation represents the functional dependence of $g(\infty)$ on the various physical parameters very well and that Eqs (44) yield a very good engineering solution for $\alpha_I(\eta^*)$.⁴⁻¹⁵

The first-order nonequilibrium solution is completed by evaluating the displacement-thickness perturbation I_I . Substitution of the foregoing solutions for $\alpha_I(\eta)$ and $g_I(\eta)$ into Eq (24b) yields

$$\begin{aligned} I_I &= - \frac{2h_D}{u_\infty^2} g(\infty) \int_0^\infty s(\eta) \left[V_s(\eta) - \frac{g(\eta)}{g(\infty)} \right] d\eta \equiv \\ &\quad - \frac{2h_D}{u_\infty^2} g(\infty) I \quad (46) \end{aligned}$$

The integral I can be regarded as independent of the surface catalyticity unless $\alpha_\infty \rightarrow 1$ or $T_w/T_0 \gtrsim 0.25$ with $\alpha_\infty > 0$. Consequently, the back effect of the nonequilibrium dissociation within the boundary layer on the self-induced pressure field is not significantly affected by the surface catalyticity unless either the freestream is highly dissociated or the wall temperature is extremely large. Typical values of I_e are presented in Table 1.

Summary of the Complete Solution

Let us now summarize the complete first-order solutions obtained for the maximum atom concentration and corresponding temperature, the induced pressure field, and the heat transfer. For this purpose, the closed-form approximations (44) previously defined will be employed (although this is, of course, not necessary). Thus, by substituting the foregoing perturbation solutions into Eqs (16c, 26, and 32), one obtains $T(\eta^*)$, p/p_∞ , and Q_w in terms of the frozen-flow solution and the nonequilibrium atom concentration as follows for a fixed wall temperature:

$$T(\eta^*) = T_F(\eta^*) - (h_D/\bar{c}_p) \times [j + (1-j)V(\eta^*)][\alpha(\eta^*) - \alpha_F(\eta^*)] \quad (47)$$

$$\frac{p_e}{p_\infty} = \left(\frac{p_e}{p_\infty}\right)_F \left\{ 1 - \frac{2h_D}{u_\infty^2} P_I \frac{I_c}{I_F} \left[\frac{\alpha(\eta^*) - \alpha_F(\eta^*)}{s(\eta^*)} \right] \right\} \quad (48)$$

$$Q_w = \left[\frac{(p_e/p_\infty)_F}{\phi_F x} \right]^{1/2} \left\{ g_F'(0) - \frac{2h_D}{u_\infty^2} \left[\frac{1-j}{v(\infty)} + P_I \frac{I_c}{I_F} g_F'(0) \right] \left[\frac{\alpha(\eta^*) - \alpha_F(\eta^*)}{\bar{s}(\eta^*)} \right] \right\} \quad (49)$$

where

$$\bar{s}(\eta^*) \equiv s(\eta^*)\{1 + j[V(\eta^*) - 1]\} \quad (50)$$

The corresponding solution for the atom concentration is given by

$$\alpha(\eta^*) - \alpha_F(\eta^*) = \Gamma g(\infty) \bar{s}(\eta^*) \quad (51)$$

with§

$$\Gamma = \Gamma_0 \phi_F \left(\frac{p_e}{p_\infty} \right)_F \times \left\{ 1 - \frac{2h_D}{u_\infty^2} z_F P_I \frac{I_c}{I_F} \left[\frac{\alpha(\eta^*) - \alpha_F(\eta^*)}{\bar{s}(\eta^*)} \right] \right\} \quad (52)$$

where $g(\infty)$ is given (approximately) by Eq (44b). These closed-form solutions, which are correct to first order in $\alpha(\eta^*) - \alpha_F(\eta^*)$ as $x \rightarrow 0$,[¶] provide useful insight as to the behavior of a nonequilibrium-dissociating boundary layer with a self-induced pressure field. Near the leading edge of the plate, for example, (51) and (52) show that the strong induced pressure field of the frozen boundary layer ($\bar{\chi}_\infty \gg 1$, $\phi_F = 2$, $\Gamma \sim 2p_0 r \bar{\chi}_\infty$) increases the atom concentration relative to the concentration predicted neglecting the induced pressure field ($\bar{\chi}_\infty = 0$, $\phi_F = 1$, $\Gamma \sim x$) by a factor $2p_0 r \bar{\chi}_\infty$. Correspondingly, Eq (48) shows explicitly that the resulting back effect of the nonequilibrium dissociation on the boundary-layer displacement thickness decreases the induced pressure below the local frozen-flow value as the dissociation level grows with increasing distance from the leading edge. This back effect grows $\sim x^{1/2}$ near the leading edge for strong interaction. Similarly, Eq (49) shows that the back effect on pressure also reduces the local heat transfer, in addition to the reduction caused by the enhanced wall enthalpy for the noncatalytic wall case. Further details of the first-order solution will be discussed in connection with some specific numerical examples.

§ Strictly speaking, the second term in Eq (52) should be dropped as second order in $\alpha(\eta^*) - \alpha_F(\eta^*)$ when used in Eq (51). However, (52) is by itself correct to first order in $\alpha(\eta^*) - \alpha_F(\eta^*)$ and will be used later in extending our solution to arbitrary degrees of dissociation.

¶ Under the original simplifying assumptions, a rigorous analysis of the present problem using power series developments of the dependent variables in $\bar{\chi}_\infty$ shows that the account of non-equilibrium effects given by these solutions is actually valid up to and including terms of order $x^{3/4}$ near the leading edge.

Table 1 Typical values of the displacement-thickness integral I : oxygen, $\omega = 1.5$, $S = 0$

M_∞	T_w/T_0	I
25	0.029	0.708
25	0.116	0.579
25	0.232	0.447
25	1.000 ^a	0.668
20	0.045	0.697
15	0.083	0.669

^a Noncatalytic wall

Extension to Arbitrary Reaction Rate

The foregoing analytical solution for $\Gamma(\xi) \ll 1$ is helpful in understanding the effects of the induced pressure field and in analyzing the initial nonequilibrium flow near the leading edge. However, the usefulness of this solution is rather limited because it usually covers only a small portion of the entire relaxation region along the plate, breaking down where nonlinear reaction-rate effects become important. Moreover, it does not prove fruitful to extend the first-order analysis by carrying the series developments (16) to higher order terms in Γ , since these higher-order corrections are very complicated and have an extremely small radius of convergence. Consequently, an approximate, nonlinear method of carrying the nearly frozen solution forward throughout the entire nonequilibrium flow field, which avoids numerical solutions of the exact nonlinear, partial differential equations of the problem, would be of interest.

Such a method was originally devised by Rae in Ref. 4 and subsequently adapted with success by the present author to several other problems involving nonequilibrium-dissociated viscous flows with both gas-phase and/or catalytic surface reactions.^{17, 18} The method is based on the intuitive notion that the nearly frozen first-order solution would still yield a reasonably good description of the nonlinear relaxation behavior as well if the reaction rate is based on the local nonequilibrium state instead of being evaluated from the frozen-flow solution. Applying this idea to the present problem, then, one assumes that Eqs (47–51), which are rigorously correct only for sufficiently small values of x , are, in fact, essentially the correct solution everywhere provided that the value of Γ from Eq (52) and the function $g(\infty)$ defined by Eq (44b) are both evaluated at the local, unknown values of $\alpha(\eta^*)$, $T(\eta^*)$, and p/p_∞ . Thus, the following is adopted as an approximate solution for the nonequilibrium atom concentration (including an induced pressure field):

$$\alpha(\eta^*) - \alpha_F(\eta^*) \simeq \Gamma \bar{s}(\eta^*) F^*[\alpha(\eta^*), T(\eta^*)] \times \{D[\alpha(\eta^*), T(\eta^*)] - R[\alpha(\eta^*), T(\eta^*), (p/p_\infty)]\} \quad (53)$$

with

$$F^*[\alpha(\eta^*), T(\eta^*)] = \frac{s(\eta^*)[v_s(\infty) - v_s(\eta^*)]}{[f''(n^*)]^2} \left[\frac{2\pi\bar{c}_p}{u_\infty^2 T_D} \right]^{1/2} T(\eta^*) \times \left\{ 1 + \operatorname{erf} \left[\frac{\eta^* f''(\eta^*) (u_\infty^2 T_D)^{1/2}}{T(\eta^*) (2\bar{c}_p)} \right] \right\} \quad (54)$$

$$D[\alpha(\eta^*), T(\eta^*)] = [1 - \alpha(\eta^*)] \times \left[\frac{T(\eta^*)}{T_{R1}} \right]^{\omega-2} \left[\frac{T(\eta^*)}{T_{R2}} \right]^S \exp \left[-\frac{T_D}{T(\eta^*)} \right] \quad (55)$$

$$R \left[\alpha(\eta^*), T(\eta^*), \frac{p_e}{p_\infty} \right] = \frac{4p_\infty/p_{at}}{A} \left[\frac{\alpha(\eta^*)^2}{1 + \alpha(\eta^*)} \right] \left[\frac{T(\eta^*)}{T_{R1}} \right]^{\omega-2} \frac{p_e}{p_\infty} \quad (56)$$

where $T(\eta^*)$ and p/p_∞ are still given by Eqs (47) and (48),

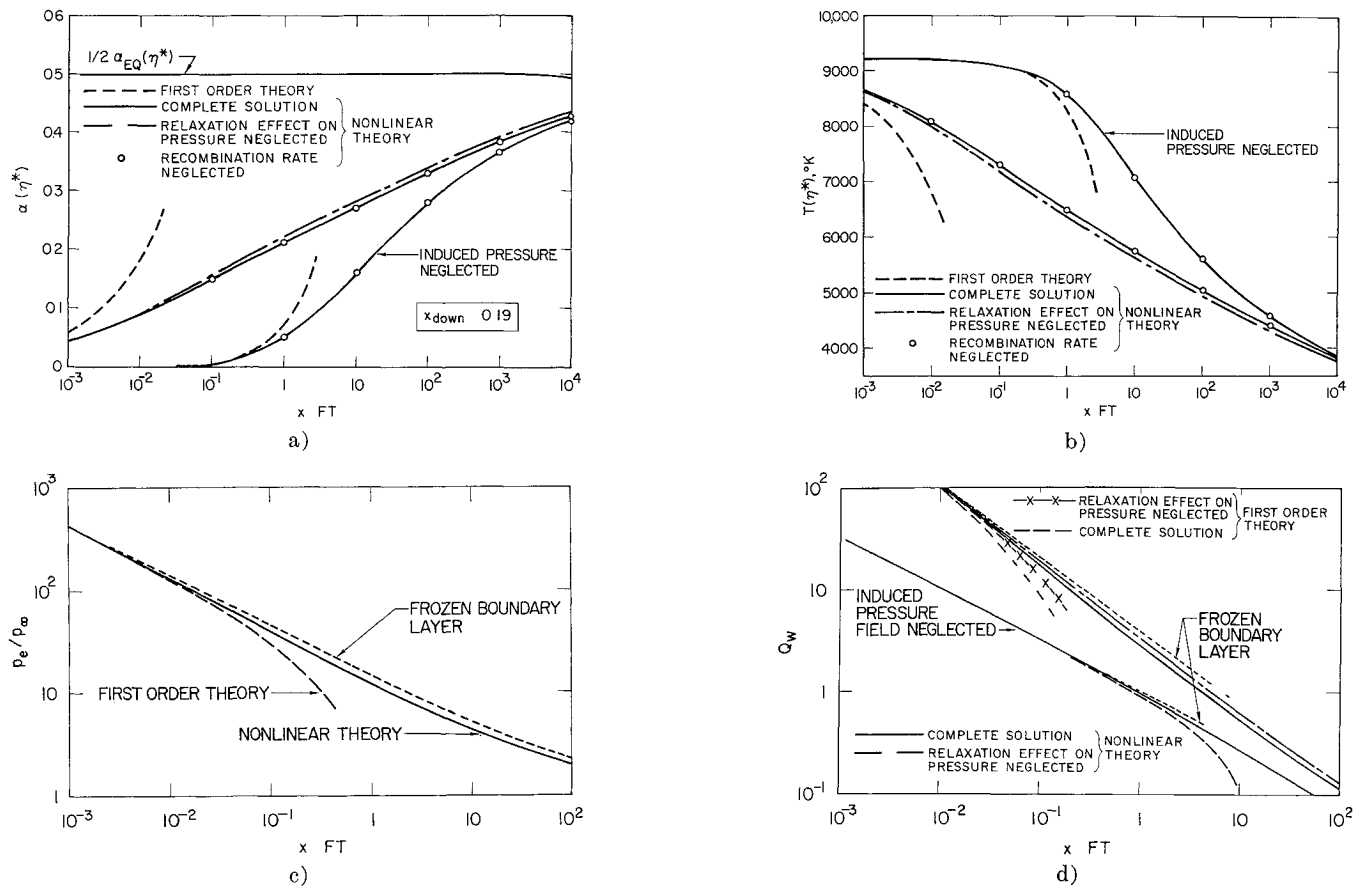


Fig. 1 Typical distributions of a) maximum atom concentration, b) maximum temperature, c) induced pressure, and d) heat transfer along a highly cooled noncatalytic plate: $M_\infty = 25$, $T_w/T_0 = 0.029$; 200,000 ft alt

respectively. Note that, in writing Eq. (53), the complete net reaction-rate function, including recombination, has been used. This is valid only when the local recombination rate is small compared to the dissociation rate, which indeed is the case until nearly complete equilibration of the dissociation reaction is reached. Moreover, retention of the recombination term ensures that $\alpha(\eta^*)$ approaches the proper functional dependence on $T(\eta^*)$ and p/p_∞ as the solution tends toward equilibrium at sufficiently large values of x , since as $x \rightarrow \infty$ the net reaction rate $D - R$ in Eq. (53) correctly approaches zero.

The foregoing approximate solution yields a set of four simultaneous nonlinear algebraic equations that are easily solved directly. By assuming a value of $\alpha(\eta^*)$ and using Eqs. (47, 48, and 54-56), Eq. (53) can be solved for $\Gamma(x)$ and the corresponding streamwise station thus determined from (52). The corresponding local nonequilibrium heat-transfer distribution can then be determined (approximately) by direct substitution into Eq. (49). Since this nonlinear solution gives the correct initial behavior in the nearly frozen-flow limit near the leading edge and also incorporates the correct qualitative behavior at large x , it should provide a fairly accurate description of the smooth, monotonic distributions of the unknowns along the plate expected in the present problem. Moreover, the proven usefulness of the extrapolation method in other applications suggests that it should provide reasonable solutions in the presence of an induced pressure field as well. To be sure, as pointed out in Ref. 4, the method does not satisfactorily describe the boundary layer all the way to equilibrium in the case of a cold wall, and further comparisons with exact solutions are certainly needed to more fully define its accuracy and limitations. Nevertheless, it appears to be quite accurate over the very highly nonequilibrium boundary-layer flow region in the vicinity

of the leading edge where the most significant induced pressures are expected to occur.

Numerical Examples

Discussion of Results

The main features of the present theory for a typical case are illustrated in Figs. 1a-1d, where distributions of $\alpha(\eta^*)$, $T(\eta^*)$, p/p_∞ , and Q_w , respectively, for the flow of oxygen over a cold, noncatalytic plate are shown with the induced pressure field both taken into account and neglected. Values of the parameters used in the present numerical examples are given in Table 2. To indicate the various operating effects, both the first-order solution and various contributions comprising the local nonlinear solution for each variable have been shown. It is seen that the first-order solutions, both with and without the induced pressure field taken into account, describe only a rather small portion of the entire nonequilibrium flow region, significantly overestimating the (nonlinear) relaxation effects beyond a local dissociation level of roughly 10%. With respect to the nonlinear solution for $\alpha(\eta^*)$, it is seen that the induced pressure field here increases the local maximum degree of dissociation in the boundary layer (relative to that predicted neglecting this field) by a factor ranging from two to three or more over the first 10-ft run of plate. This increase in $\alpha(\eta^*)$ also causes a pronounced reduction of the local maximum temperature (e.g., by 1300°K at $x = 10$ ft) because of the large dissociation energy involved. The corresponding back effect of the nonequilibrium dissociation on the displacement thickness reduces the local induced pressure field about 20% below that computed for a frozen boundary-layer flow, resulting in a slightly more rapid pressure decay downstream of the leading edge. Also,

Table 2 Values of parameters used in example calculations (1958 revised ARDC model atmosphere)

Gas: oxygen	
h_d	$= 1\,649 \times 10^8 \text{ ft}^2/\text{sec}^2$
T_d	$= 59,000^\circ\text{K}$
ω	$= -1.5$
S	$= 0$
T_1	$= 4500 \text{ K}$
k'	$= 5 \times 10^{14} \text{ cm}^5/\text{mole}^2\text{-sec}$
\bar{c}_p	$= 9800 \text{ ft}^2/\text{sec}^2\text{-}^\circ\text{K}$
α_∞	$= 0$
C_∞	$= 1$
A	$= \exp 16$
$\bar{\gamma}_\infty$	$= 1.40$

Fig 1d shows that the reduction in heat transfer caused by nonequilibrium dissociation grows more rapidly downstream of the leading edge when the induced pressure field is taken into account, with about half of this enhanced reduction resulting from the back effect of the nonequilibrium dissociation on the pressure field itself. However, it is seen that this back effect has a negligible effect on both $\alpha(\eta^*)$ and $T(\eta^*)$ throughout the relaxation region, which was generally found to be the case in all the numerical examples presented here.

The effect of flight altitude at $M_\infty = 25$ on the distributions of atom concentration and pressure along the plate is shown in Figs 2a and 2b, respectively, for a highly cooled noncatalytic wall**. It is seen that increasing altitude enhances the relative effect of the induced pressure field on the nonequilibrium dissociation within the boundary layer because of a lower Reynolds number, although the dissociation level itself is decreasing, since the reduced ambient density decreases the dissociation rate. From the results presented in Figs 1 and 2 plus other examples computed,¹⁴ it appears that the induced pressure field can have a significant effect on the nonequilibrium flow field along the first 10 ft of a highly cooled plate throughout the altitude range of 150–300 kft for flight Mach numbers in excess of 20. At lower flight speeds in this altitude range, however, the initial dissociation rate within the boundary layer (even including the effect of the induced pressure field) is so small that the boundary layer will remain completely frozen over plate lengths of practical interest unless $T_w/T_0 \gtrsim 0.25$.

In all cases where the induced pressure field has a significant effect on the nonequilibrium flow in the boundary layer, it is seen that most of this effect occurs in the strong interaction region. By the time the decaying induced pressure ratio $(p/p_\infty) - 1$ drops to values of order unity or less (moderate to weak interaction regime), the difference between the solutions obtained by either including or neglecting the induced pressure field has already become comparatively small. This result justifies the use of Eq (15) as a model of the pressure field for the purposes of the present investigation. The moderate-to-weak interaction regime tends to occur where the boundary layer has already relaxed appreciably away from the initial frozen state and would appear to be of interest mainly in connection with a nearly or completely equilibrated flow.

It should also be noted that the effect of the gas-phase recombination rate on each of the solutions presented here was found to be completely negligible, as is illustrated, for example, in Fig 1a. This is not surprising since, as previously pointed out, the dissociation rate is known to be the controlling reaction in a highly dissipative nonequilibrium boundary layer until the flow approaches very close to equilibrium.^{3,4} As may be seen in Figs 1 and 2, the boundary layer is indeed far from equilibrium throughout, the

maximum atom concentrations remaining well below the equilibrium values $\alpha_q(\eta^*)$ corresponding to the local $T(\eta^*)$ for distances up to $x = 10^4$ ft.

Significance of the Fully Viscous Region

According to the present strong interaction theory, the large self-induced pressures occurring near the leading edge of a flat plate in hypersonic flow can significantly enhance the dissociation rate and nonequilibrium atom concentration (and reduce the temperature) within the boundary layer for flight conditions of practical interest. However, as shown by the foregoing representative results, the theory predicts that a good deal of the induced pressure field effect on the nonequilibrium relaxation takes place extremely close to the leading edge, where the strong interaction theory undoubtedly breaks down because of the presence of a fully viscous shock layer. Therefore, in concluding, it is of interest to define more precisely where the present analysis fails in this respect, using a rough estimate of the upstream limit of the strong interaction theory (downstream limit of the fully viscous theory) due to Oguchi.¹⁹ Equating the pressure obtained from an analysis of the wedge-like fully viscous region for frozen flow to the pressure given by strong interaction theory, he finds that the latter theory should be (roughly) applicable beyond a certain distance x_{dwn} given by

$$(\tilde{x}_\infty)_{dwn} \approx \left(\frac{\tilde{x}_\infty - 1}{2p_0 F} \right) M_\infty^2 G \quad (57)$$

where G is a function of the wall temperature ratio T_w/T_0 alone (see Ref 19) ranging from a value of 0.25 for a highly cooled wall to 0.80 for an adiabatic wall with $Pr = 1$ and a linear viscosity-temperature relation. Using Eq (57), the values of x_{dwn} appropriate to each of the numerical examples pre-

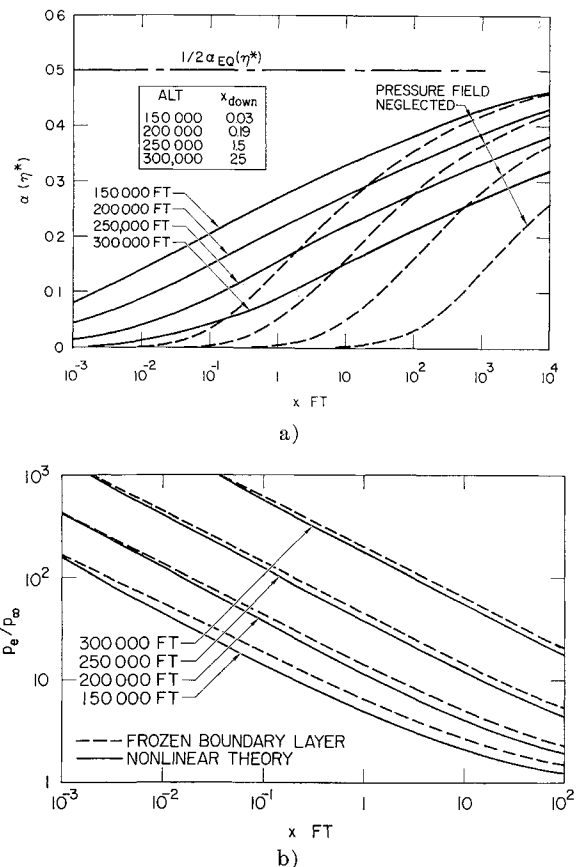


Fig 2 Effect of altitude on a) maximum atom concentration and b) induced pressure along a noncatalytic plate: $M_\infty = 25$, $T_w = 1000 \text{ K}$

** Additional numerical results showing the effects of Mach number, surface catalycity, and wall temperature can be found in Ref 14.

sented here have been computed and are indicated on Figs 1 and 2. Now, from the solutions obtained with the induced pressure field neglected, one would conclude that the nonequilibrium boundary-layer relaxation begins essentially downstream of the fully viscous flow region for all the flight conditions shown in these figures. On this basis, the boundary-layer theory would be acceptable for analyzing the nonequilibrium aspects of the flow problem and the more difficult, fully viscous region could be treated as a chemically frozen (perfect-gas) problem. However, upon taking the effect of the induced pressure field into account according to strong interaction theory, it is seen instead that a considerable degree of nonequilibrium dissociation occurs in the fully viscous flow region where the strong interaction theory breaks down. As expected, Fig 2 shows that an increasingly greater portion of the significant induced pressure-field effect on chemical relaxation falls within this viscous region with increasing altitude.

On the basis of the foregoing estimates, it is clear that the strong interaction boundary-layer theory overestimates the effect of the strong induced pressure field on the nonequilibrium boundary-layer relaxation along a flat plate. This is because the induced pressure field involved increases without limit ($\sim x^{-1/2}$) as the leading edge is approached and thus gives too high a pressure (and dissociation rate) at sufficiently small values of x , whereas there actually occurs a leveling-off of the pressure to a certain plateau value as $x \rightarrow 0$ because of the wedge-like action of the fully viscous region.^{14-19, 20} In this respect, the present theory serves as a useful upper limit in determining the effects of the induced pressure field on the nonequilibrium viscous flow along the plate. Moreover, since the induced pressure at the leading edge plateau can be quite large under the hypersonic, high-altitude flight conditions considered, there could still be a significant enhancement of the dissociation over the plate even when a more realistic model of the pressure field that includes the effect of the fully viscous flow region is used. If this indeed be the case, then the fully viscous region itself could contain nonequilibrium dissociation and would not be satisfactorily regarded as a chemically frozen flow.

References

- ¹ Liu, J. T. C., "On the role of high temperature effects on heat transfer in hypersonic viscous interaction," *Developments in Mechanics* (Plenum Press, Inc., New York, 1961), Vol. 1, pp. 417-429.
- ² Mann, W. M., Jr. and Bradley, R. G., Jr., "Hypersonic viscid-inviscid interaction solutions for perfect-gas and equilibrium real-air boundary layer flow," *Advances in Astronautics* (Plenum Press, Inc., New York, 1963), Vol. 8, pp. 198-217.
- ³ Gibson, W. E., "Dissociation scaling for the nonequilibrium blunt-nose flows," *ARS J.* **32**, 285-286 (1962).
- ⁴ Rae, W. J., "A solution for the nonequilibrium flat plate boundary layer," *AIAA J.* **1**, 2279-2289 (1963).
- ⁵ Lees, L., "On the boundary layer equations in hypersonic flow and their approximate solution," *J. Aeronaut. Sci.* **20**, 143-145 (1953).
- ⁶ Lees, L., "Laminar heat transfer over blunt-nosed bodies at hypersonic flight speeds," *Jet Propulsion* **26**, 259-269 (1956).
- ⁷ Cheng, H. K., Hall, J. G., Golian, T. C., and Hertzberg, A., "Boundary layer displacement and leading edge bluntness effects in high temperature hypersonic flow," *J. Aerospace Sci.* **28**, 353-381 (1961).
- ⁸ Moore, F. K., "On local flat plate similarity in the hypersonic boundary layer," *J. Aerospace Sci.* **28**, 753-762 (1961).
- ⁹ Penner, S. S., *Chemistry Problems in Jet Propulsion* (Pergamon Press, New York, 1957), pp. 216-232.
- ¹⁰ Hall, J. G., Eschenroeder, A. Q., and Marrone, P. V., "Blunt-nose inviscid airflows with coupled nonequilibrium processes," *J. Aerospace Sci.* **29**, 1038-1052 (1962).
- ¹¹ Wray, K. L., "Chemical kinetics of high temperature air," *AIAA Progress in Astronautics and Rocketry: Hypersonic Flow Research*, edited by F. R. Riddell (Academic Press Inc., New York, 1962), Vol. 7, pp. 181-204.
- ¹² Hayes, W. D. and Probstein, R. F., *Hypersonic Flow Theory* (Academic Press Inc., New York, 1959), p. 280.
- ¹³ Dewey, C. F., Jr., "Use of local similarity concepts in hypersonic viscous interaction problems," *AIAA J.* **1**, 20-33 (1963).
- ¹⁴ Inger, G. R., "Nonequilibrium hypersonic boundary layer flow along a sharp flat plate with a strong induced pressure field," *AIAA Preprint* 63-442 (August 1963).
- ¹⁵ Inger, G. R., "Highly-nonequilibrium boundary layer flows of a multicomponent dissociated gas mixture," *Aerospace Corp. Rept. TDR-269 (4230-10)-2* (October 1963).
- ¹⁶ Morse, P. M. and Feshbach, H., *Methods of Theoretical Physics* (McGraw-Hill Book Co., Inc., New York, 1953), pp. 440-442.
- ¹⁷ Inger, G. R., "Nonequilibrium-dissociated stagnation point boundary layers with arbitrary surface catalyticity," *AIAA J.* **1**, 1776-1784 (1963).
- ¹⁸ Inger, G. R., "Dissociated laminar boundary layer flows over surfaces with arbitrary continuous distributions of catalyticity," *Intern. J. Heat Mass Transfer* **6**, 815-832 (1963).
- ¹⁹ Oguchi, H., "The sharp leading edge problem in hypersonic flow," *Brown Univ. Div. Eng. Rept., Aeronaut. Res. Lab., ARL TN 60-133* (1960).
- ²⁰ Nagamatsu, H. T. and Sheer, R. E., Jr., "Hypersonic shock wave-boundary layer interaction and leading edge slip," *ARS J.* **30**, 454-462 (1960).